

Phylogeography of *Lasiopodomys gregalis* (Rodentia: Cricetidae) in the southern part of its geographic range

Tatyana V. Petrova*, Alexander N. Kuksin, Nikolay I. Putintsev,
Natalia V. Lopatina & Andrey A. Lissovsky*

ABSTRACT. The narrow-headed vole species complex (subgenus *Stenocranius*) is represented by at least two cryptic species: *Lasiopodomys gregalis* and *L. raddei*. One of *L. gregalis* lineages (lineage B, inhabiting northern Mongolia and neighbouring territories) forms a secondary contact zone with *L. raddei*. In the current study, we analysed phylogeographic structure of *L. gregalis* lineage B by means of sequences of mitochondrial cytochrome *b* and reconstructed ecological niches of both species at present and in the past. The source of the spread of *L. gregalis* lineage B was probably the territory of modern western Mongolia and southeastern Tuva. Despite seeming continuity of the geographic range of lineage B, mitochondrial clusters within it turned out to be allopatric or parapatric; the reasons for such spatial structure are not yet clear. Based on the ecological niche modelling, it can be hypothesised that the two studied species reacted differently to climatic fluctuations of the late Pleistocene, and the structure of the modern geographic range of *L. gregalis* lineage B has formed largely due to inter-specific competitive interactions with *L. raddei*.

How to cite this article: Petrova T.V., Kuksin A.N., Putintsev N.I., Lopatina N.V., Lissovsky A.A. 2023. Phylogeography of *Lasiopodomys gregalis* (Rodentia: Cricetidae) in the southern part of its geographic range // Russian J. Theriol. Vol.22. No.2. P.102–119. doi: 10.15298/rusjtheriol.22.2.03

KEY WORDS: ecological niche modelling, cytochrome *b*, narrow-headed vole, *Stenocranius*, *Lasiopodomys raddei*

Tatyana V. Petrova [p.tashka@inbox.ru], Zoological Institute of Russian Academy of Sciences, Universitetskaya Emb. 1, Saint-Petersburg 199034, Russia; Alexander N. Kuksin [kuksintuva@yandex.ru], Tuvian Institute for Exploration of Natural Resources, Siberian Branch of Russian Academy of Sciences, Internatsionalnaya Str. 117a, Kyzyl 667007, Russia; Nikolay I. Putintsev [niputin@mail.ru], Tuvan State University, Lenina Str. 36, Kyzyl 667000, Russia; Nataliya V. Lopatina [lopatinanata@yandex.ru], Institute of Systematics and Ecology of Animals, Siberian Branch of Russian Academy of Sciences, Frunze Str. 11, Novosibirsk 630091, Russia; Andrey A. Lissovsky [andlis@zmmu.msu.ru], A.N. Severtsov Institute of Ecology and Evolution, Russian Academy of Sciences, Leninsky Prospekt 33, Moscow 119071, Russia.

Филогеография *Lasiopodomys gregalis* (Rodentia: Cricetidae) в южной части ареала

Т.В. Петрова*, А.Н. Куксин, Н.И. Путинцев, Н.В. Лопатина, А.А. Лисовский*

РЕЗЮМЕ. Комплекс видов узкочерепных полевок (подрод *Stenocranius*) представлен по крайней мере двумя криптическими видами — *Lasiopodomys gregalis* и *L. raddei*. Одна из линий *L. gregalis* (линия В, населяющая северную Монголию и соседние территории) формирует вторичную зону контакта с *L. raddei*. В рамках данной работы мы анализировали филогеографическую структуру генетической линии В *L. gregalis* на основании последовательностей митохондриального гена цитохрома *b*, а также реконструировали экологические ниши обоих видов в настоящем и в прошлом. Источником расселения линии В *L. gregalis*, вероятно, была территория современной западной Монголии и юго-восточной Тувы. При кажущейся непрерывности ареала линии В, митохондриальные кластеры внутри неё оказываются аллопатричны или парapatричны, причины такой пространственной структуры пока не ясны. По результатам моделирования экологических ниш можно предположить, что исследуемые виды реагировали на климатические флуктуации позднего плейстоцена различным образом, и структура современного ареала линии В *L. gregalis* сформировалась во многом благодаря межвидовым конкурентным взаимодействиям с *L. raddei*.

КЛЮЧЕВЫЕ СЛОВА: моделирование экологической ниши, цитохром *b*, узкочерепная полевка, *Stenocranius*, *Lasiopodomys raddei*.

* Corresponding author

Introduction

Narrow-headed voles (subgenus *Stenocranius*) are a widespread rodent species complex inhabiting dry open landscapes: tundra, steppe and alpine meadows. During the Pleistocene, this complex's geographic range was continuous, occupied the territory covered by tundra-steppe and steppe and extended almost to the entire territory of the northern Palearctic. With the formation of a wide taiga zone in the Holocene, its geographic range broke up into several isolated regions. Narrow-headed voles' evolutionary history has been thoroughly discussed in the context of climatic fluctuations (Prost *et al.*, 2013; Baca *et al.*, 2019; 2023).

Based on molecular, craniological and breeding data (Petrova *et al.*, 2016), it has been shown that the narrow-headed vole species complex is represented by at least two closely related species — widespread *Lasiopodomys gregalis* (Pallas, 1779), as well as *L. raddei* (Poljakov, 1881), which occurs locally in southeastern Transbaikalia; the two probably diverged at the beginning of the Middle Pleistocene, ~0.8 Mya (Petrova *et al.*, 2015).

Lasiopodomys gregalis consists of three strongly diverged mitochondrial lineages: A, B and C (Petrova *et al.*, 2015). Recently, in a microsatellite loci analysis, it was demonstrated that these lineages are not an artefact of the mitochondrial-DNA distribution. According to species distribution modelling (SDM) results, they are potentially able to come into contact in the Altai-Sayan region but are still genetically isolated, and therefore can be recognised as separate taxa, probably of the lowest taxonomic rank (Petrova *et al.*, 2021). Judging by our previous findings (Petrova *et al.*, 2015), the common ancestor of the three *L. gregalis* lineages inhabited the Altai-Sayan region, where subsequent separation of three lineages A, B and C occurred. Palaeontological data indirectly support the hypothesis of the *L. gregalis* sensu lato ancestral range: a sister lineage of the most recent common ancestor (MRCA) of the three *L. gregalis* lineages was discovered by Baca *et al.* (2023) in Denisova Cave (Altai).

The narrow-headed vole was the most abundant and common mammalian species in all habitats throughout Eurasia in the Late Pleistocene and was tightly associated with the mammoth faunistic complex (Gerasimov & Velichko, 1982; Kowalski, 2001; Markova & van Kolfshoten, 2008). According to dental morphology of the narrow-headed vole, even stratigraphic horizons can be distinguished. Therefore, it is especially important to understand in detail the evolutionary history of this interesting wide-ranging and ecologically diverse species. Previous studies (Prost *et al.*, 2013; Petrova *et al.*, 2015) have mainly been focused on lineage A, whose geographic range underwent fragmentation caused by the expansion of forests in the Holocene. Lineage C is an endemic of central Tuva and has a narrow range. The third one, lineage B, occurs in arid areas across Mongolia from Lake Uvs-Nuur in the west to eastern Transbaikalia and middle reaches of the Amur River. Phylogeographic structure of this lineage was studied preliminarily (Petrova *et al.*, 2015), whereas

new genetic data (Petrova, 2017; Petrova *et al.*, 2016; 2021; 2023) indicate that lineage B itself also has well-pronounced phylogeographic structure.

The uniqueness of the Southern Siberia territory is the ecotonicity in both latitudinal and longitudinal directions. Southern Siberia is the boundary between boreal and arid regions of the Holarctic and at the same time a transitional band at the junction of the ultra-continental and continental sectors of the Palearctic (Karamysheva, 1988). The buffer position of this territory manifests itself, among other things, in the complexity and originality of the flora. The mountain belt of Southern Siberia (Altai-Sayan-Baikal mountain country) is an area with the richest floral biodiversity, in particular steppe biocoenoses (Namzalov, 2021), which are the main biotope of the narrow-headed vole in the southern part of its geographic range. Zonation structure of Southern Siberia is determined by the location of mountain ranges, uplands and intermontane basins in different climatic facies. Thus, steppe communities are fragmented and in particular are observed in the extra-zonal steppe formations located on warm insulated slopes (Makunina *et al.*, 2007; Namzalov, 2020).

As revealed recently (Petrova *et al.*, 2023), ecological preferences in Transbaikalia differ significantly between *L. gregalis* lineage B and *L. raddei*, although these preferences are caused by the same environmental factors. This finding led us to the idea of the importance of understanding the evolutionary history of lineage B: this task may be key to the elucidation of the mechanisms behind parapatric co-occurrence of the two species in Transbaikalia. Accordingly, this study is devoted to reconstruction of the evolutionary history of *L. gregalis* lineage B using mitochondrial cytochrome *b* (mt *cytb*) data and new direct calibrations for divergence dating and SDM.

Material and methods

Sampling, DNA isolation and mitochondrial cytochrome b amplification

In total, 137 narrow-headed voles of lineage B from 47 localities in southeastern Tuva, Zabaikalskiy Territory and Amur Region of Russia and in northern Mongolia were included in the molecular analysis. Sequences from 29 specimens were obtained within the framework of the current study; the rest were downloaded from the NCBI Nucleotide database or taken from our previous studies (Fig. 1, Appendix 1). Additionally, to perform the divergence dating analysis, we used mt *cytb* sequences of the two other lineages (A and C) of *Lasiopodomys gregalis* and of *L. raddei* published before (Petrova *et al.*, 2015; 2023) along with sequences of *L. gregalis* from Denisova Cave (Altai) and radiocarbon-dated *Lasiopodomys anglicus* Hinton, 1910, from Late Pleistocene Europe (Baca *et al.*, 2023).

Isolation of genomic DNA from fresh muscle tissue samples stored in 96% ethanol was performed with the ExtractDNA Blood & Cells Kit (Evrogen, Russia). DNA from museum skin samples was extracted using

the QIAmp Tissue Kit (Qiagen). To reduce potential contamination, all manipulations with the museum specimens were carried out in a separate laboratory room isolated from the post-PCR facilities that are predominantly being used for studies on historical samples from the collection at the Zoological Institute of RAS. All the working surfaces, instruments and plasticware were sterilised with UV light and chloramine-T.

A part of the *cytb* gene was amplified with primers UCBU and LM by a standard protocol described elsewhere (Abramson *et al.*, 2009). To amplify short overlapping *cytb* fragments from museum skin samples, we used five pairs of primers generated in our previous study (Petrova *et al.*, 2015).

Sequences obtained in the current study were submitted to GenBank under the following accession numbers: OR004258–OR004286 (Appendix 1).

Phylogenetic analyses

Sequences were edited and aligned with the CLUSTALW algorithm (Thompson *et al.*, 1994) implemented in BioEdit (Hall, 1999). The level of genetic differentiation in *cytb* on the basis of *p*-distances was estimated in MEGA 7.0.18 (Kumar *et al.*, 2016).

We employed PartitionFinder 2.1.1 (Lanfear *et al.*, 2017) involving AICc (corrected Akaike information criterion) and the ‘user’ algorithm to select an optimal partitioning scheme: either separate models for a codon position (1, 2, 3 or 1+2, 3) or analysis without any partitioning. The latter analysis was chosen as the ‘best scheme’ with the GTR+I+G+X model.

Phylogenetic reconstruction based on *cytb* sequences was performed using 135 specimens of *L. gregalis* lineage B, whereas specimens of lineages A and C and of *L. raddei* served as an outgroup. The final alignment comprised a 1018-bp *cytb* fragment. Maximum likelihood (ML) analysis was performed on the IQ-TREE Web server (Trifinopoulos *et al.*, 2016) with 10,000 ultrafast bootstrap replicates (Hoang *et al.*, 2018). Bayesian inference (BI) analysis was carried out in MrBayes 3.2.6 (Ronquist *et al.*, 2012) with the following parameters: nst = mixed and the distribution of the substitution rates between sites; the dataset was divided into partitions by codon position. Each analysis was started with a random tree and involved two replicates with four Markov chains (MCMC) for 3 million generations each, with the results recorded every 1000th generation. Stationarity and convergence of separate runs were assessed using ESS statistics in Tracer v1.7 (Rambaut *et al.*, 2018). A maximum clade credibility tree was constructed based on the trees sampled after 25% burn-in and was visualised by means of the FigTree v1.6 software (<http://tree.bio.ed.ac.uk/software/figtree/>, accessed on 26 November 2021).

The phylogenetic network for *L. gregalis cytb* data was computed via the median-joining algorithm implemented in PopART 1.7 (<https://popart.maths.otago.ac.nz>). The alignment used for the network analysis and for calculation of genetic diversity indices was truncated to the length of shorter sequences (with the final length

comprising the 776 bp fragment) and included 128 sequences (several museum specimens were excluded due to insufficient sequence length). Genetic diversity indices and haplotype (H_d) and nucleotide (P_i) diversity levels along with their standard deviations within seven major *cytb* haplogroups of *L. gregalis* and *L. raddei* were calculated in DNASP v6.12 (Rozas *et al.*, 2017).

Divergence dating

Divergence time points within *Lasiopodomys voles* phylogeny were estimated by the Bayesian relaxed-clock method in the BEAST v2.6.7 software (Bouckaert *et al.*, 2014). We analysed an expanded *cytb* alignment that included specimens of lineages A and C of *L. gregalis* and of *L. raddei*. For more accurate dating, we also utilised 11 *cytb* sequences of *L. anglicus* from Late Pleistocene Europe (all the radiocarbon-dated specimens) and five sequences of *L. gregalis* from Denisova Cave, as published by Baca *et al.* (2023). These sequences were dated in terms of tip dates according to radiocarbon dates of *L. anglicus* (14.26–42.64 thousand years ago, kya) or results of those authors’ molecular dating for *L. gregalis* (26.477–113.05 kya). To calibrate the tree root, we added the following outgroup specimens too: *Lasiopodomys brandtii* (Radde, 1861) (GenBank accession No. JF906120), *L. mandarinus* (Milne-Edwards, 1871) (FJ986322), *Alexandromys kikuchii* (Kuroda, 1920) (NC_003041), *Neodon fuscus* (Büchner, 1889) (NC_040138) and *Chionomys nivalis* (Martins, 1842) (MT381934). The MRCA of the ‘*Microtus*’ species group (all taxa excluding the genus *Chionomys*) was calibrated by means of a normal distribution, with a mean of 2.2 Mya based on the assumption of Late Pliocene radiation of basal lineages of ‘*Microtus*’ (Tesakov *et al.*, 1999; Zheng & Zhang, 2000; Martin *et al.*, 2008) and 0.2 Mya as its standard error according to Bannikova *et al.* (2010). The GTR+I+G substitution model, empirical base frequencies and a relaxed log-normal clock with the coalescent constant population model were applied as a tree prior.

Species distribution modelling

We assessed temporal range shifts of *L. gregalis* lineage B and of *L. raddei* by building last interglacial (LIG, 140–120 kya), last glacial maximum (LGM, ~21 kya), and present species distribution models. Bioclimatic variables of WorldClim and elevational grids of 0.02-degree spatial resolution served as ecological predictors (Fick & Hijmans, 2017; Karger *et al.*, 2017). We did not find an elevation grid for the LIG, and therefore we used the LGM grid in this analysis. Species occurrences were mainly taken from the information on the molecular voucher specimens (Fig. 1). To reduce spatial autocorrelation and sampling bias, we excluded duplicated localities within a 50-km resolution grid and controlled Moran’s I after each modelling run. The test sample was obtained by rarefaction of the initial dataset via a similar procedure, but the grid resolution and rarefying distance were 1.1-fold greater.

We chose the ‘maxent.jar’ algorithm implemented in the ENMeval 2.0.3 R package (Muscarella *et al.*,

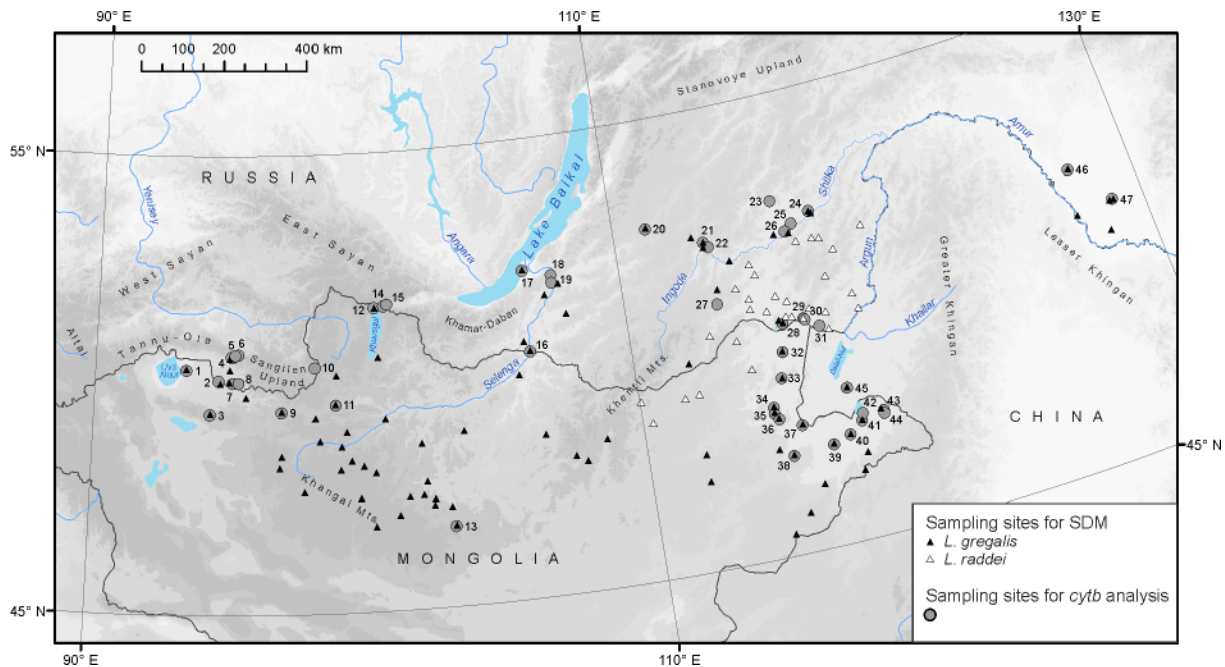


Fig. 1. Sampling sites of *Lasiopodomys gregalis* lineage B. Samples subjected to the cytochrome *b* analysis are marked with grey circles, and the locality ID numbers correspond to Appendix 1. Samples used for SDM are indicated by triangles: black for *L. gregalis* and white for *L. raddei*.

2014; Kass *et al.*, 2021) to build Maxent models with a set of parameters by means of regularisation multipliers ranging from 0.75 to 3 with three combinations of feature classes (L, LQ and LQH where L = linear, Q = quadratic and H = hinge). For the final analysis, we selected only those predictors whose permutation importance was above 2% in the preliminary runs. The best model was chosen based on the AICc calculated by means of the test sample. Ten thousand background points were randomly selected for model calculation from the whole study territory with a slightly (two-fold) higher probability of point selection outside a 40 km buffer area around voles' occurrence points.

Results

Phylogenetic analyses

The result of tree reconstruction was overall consistent with our previous study (Petrova *et al.*, 2015) and showed subdivision of lineage B into western, Transbaikalian and Amur sub-lineages, but the additional data made the phylogenetic structure of *L. gregalis* more complicated (Figs 2, 3). The western part of the *L. gregalis* lineage B distribution is represented by four clusters B1–B4 and is basal towards the eastern one. Cluster B1 is composed of specimens from southeastern Tuva and western Mongolia (localities 1–3 and 8–11) and is basal to the whole lineage B. Cluster B2 consists of specimens from southeastern Tuva, mainly from the Eastern Tannu-Ola Mountain Range (localities 4–7). Cluster B3

from the northern shore of Lake Khuvsgul (locality 12) is grouped with moderate support ($bpv = 0.89$, $bs = 90.0$) with the B2 cluster. Two specimens from central Mongolia (locality 13) constitute cluster B4. Two major branches can be distinguished within the eastern clade. The first one is formed by clusters B5 and B6 from Transbaikalia and eastern Mongolia, respectively, whereas the populations of eastern Mongolia are subsidiaries of the populations of Transbaikalia. The second branch of the eastern lineage is composed of specimens from the middle Amur River, cluster B7 (localities 46 and 47).

Intergroup *p*-distances based on *cytb* data (Tab. 1) varied from 0.9–1.5% (between populations of southeastern Tuva and western and central Mongolia: clusters B1–B4) to 1.0–2.5% (between populations of the eastern part of the geographic range: the middle Amur River and Transbaikalia, i.e. clusters B5–B7) and 1.8–3.2% (between western and eastern populations), whereas populations of southeastern Tuva and western Mongolia (B1) and eastern Mongolia (B6) are the most distant ones.

The median-joining haplotype network (Fig. 3A) contains a hypothetical 'central' node (marked with an asterisk), branches from which lead to four geographical groupings from western and central Mongolia and southeastern Tuva (clusters B1–B4) and to the fifth one: the 'common ancestor' of the eastern lineage (clusters B5–B7). The network does not indicate a united position of cluster B2 from southeastern Tuva (Tannu-Ola) with cluster B3 formed by specimens from the northern shore of Lake Khuvsgul, as displayed in the phylogenetic tree. The haplotype that

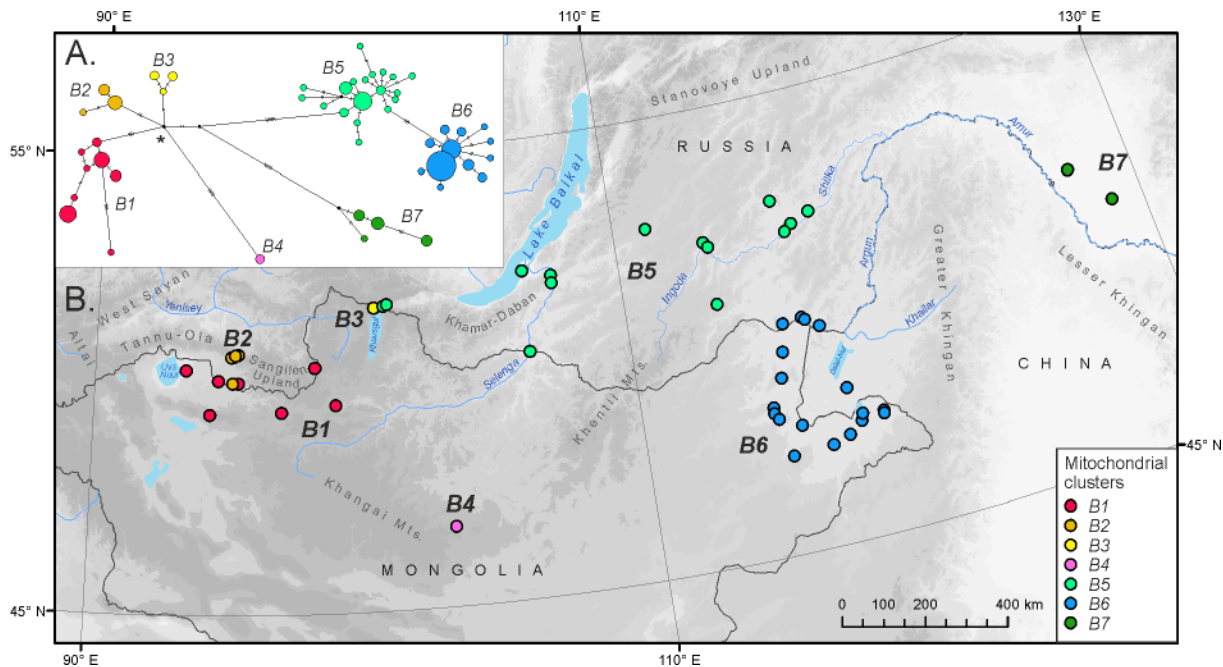


Fig. 3. A: The median-joining haplotype network based on cytochrome *b* data of *Lasiopodomys gregalis* lineage B. The size of the circles is proportional to haplotype frequency; branch length is scaled and shown with hatch marks. B: The geographic distribution of mitochondrial clusters.

contrary, the eastern Mongolian cluster (B6), which is a subsidiary of cluster B5, has star-like structure with two shared haplotypes occurring each in five and 11 localities throughout eastern Mongolia and bordering regions of southeastern Transbaikalia.

Haplotype diversity (H_d) within three major haplogroups (Tab. 2) varies from 0.639 in the Tannu-Ola cluster (B2) and 0.748 in *L. raddei* to 0.926 in Transbaikalia (B5). Nucleotide diversity (P_i) varies from 0.12–0.18% in clusters B2 and B3 (Tannu-Ola and

Table 1. Average p-distances between (below diagonal) and within populations (diagonal) according to cytochrome *b* data

Mitochondrial cluster	B1	B2	B3	B4	B5	B6	B7
B1. Southeastern Tuva, western Mongolia	0.004						
B2. Southeastern Tuva, Tannu-Ola	0.014	0.001					
B3. Lake Khuvsgul	0.013	0.009	0.001				
B4. Central Mongolia	0.015	0.012	0.011	0.001			
B5. Transbaikalia	0.026	0.022	0.023	0.025	0.003		
B6. Eastern Mongolia	0.032	0.027	0.026	0.031	0.010	0.002	
B7. Amur	0.023	0.019	0.018	0.020	0.020	0.025	0.003

Table 2. Genetic diversity within the major haplogroups. *n*, sample size; *h*, the number of haplotypes; H_d , haplotype diversity; P_i , nucleotide diversity; SD, standard deviation.

Mitochondrial cluster / species	<i>n</i>	<i>h</i>	H_d (SD)	P_i (SD)
B1. Southeastern Tuva, western Mongolia	22	8	0.827 (0.052)	0.31 (0.04)
B2. Southeastern Tuva, Tannu-Ola	9	3	0.639 (0.126)	0.12 (0.04)
B3. Lake Khuvsgul	5	3	0.800 (0.164)	0.15 (0.04)
B4. Central Mongolia	2	1	n/a	n/a
B5. Transbaikalia	33	19	0.926 (0.032)	0.30 (0.04)
B6. Eastern Mongolia	46	12	0.756 (0.056)	0.18 (0.02)
B7. Amur	11	4	0.782 (0.075)	0.29 (0.06)
<i>L. raddei</i>	67	22	0.748 (0.056)	0.26 (0.03)

Khuvsgul groups) to 0.31% in cluster B1 (western Mongolia). The highest nucleotide diversity was found in the B1 cluster from southeastern Tuva and western Mongolia (Tab. 2), indicating the absence of sharp fluctuations in population size.

Cytochrome *b* genotyping

One of the aims of the current study was to determine genetic affiliation of several specimens from previously unexplored territories. The new material from the Tunka basin is represented by only two museum specimens (Fig. 1, localities 14 and 15), for which only short fragments of mt *cytb* (160 bp) have been obtained so far. We did not include them in the final versions of the phylogenetic and population analyses owing to their insufficient length. Nonetheless, the alignment and preliminary phylogenetic reconstruction identified them clearly as members of lineage B and identical to specimens from Transbaikalia and eastern Mongolia.

Additionally, we checked our earlier conclusion (Petrova *et al.*, 2015; 2021) about the sympatry of *L. gregalis* lineages B and C in Tuva in the vicinity of the Ust-Buren Village. It was found that this information emerged due to an error in the materials' labels. The collector's diary contains information about four specimens from that expedition: three from Ust-Buren (lineage C geographically speaking) and one from the Erzinsky District (lineage B geographically). These four specimens are stored in the Zoological Museum of Moscow State University with correct labels. The error came from labels of three tissue samples that are stored separately in the Zoological Institute RAS tissue collection: all of them are labelled as Ust-Buren. We compared *cytb* sequence of the specimen that was found to belong to lineage B from this group of tissue samples — with *cytb* of a voucher specimen (ZMMU S-188787) from the Erzinsky District of Tuva (Fig. 1, loc. 7) and found them genetically identical. Thus, we concluded that our hypothesis of the sympatry of two genetic lineages in Ust-Buren was erroneous due to tissue mislabelling. We updated geographic information in the NCBI Nucleotide database (accession No. KJ192307) accordingly.

Divergence dating

This analysis based on *cytb* sequences (Fig. 4) indicated the polytomy of *L. anglicus*, *L. raddei* and of a branch leading to the MRCA of *L. gregalis*; *L. anglicus* is grouped together with *L. raddei*, albeit with low support (bpp = 0.64). The MRCA of these basal lineages of the subgenus *Stenocranius* dates back to the Middle Pleistocene, ~652 kya (Tab. 3). Taking into account the addition of molecular data from layers 12.3 and 14 of Denisova Cave, the order of basal branches within *L. gregalis* is unresolved: the cluster uniting representatives of lineages A, B and C of *L. gregalis* is unsupported (bpp = 0.54). Lineages A and B+C split ~346 kya, whereas the MRCA of lineages B and C dates back to ~259 kya, and the first subdivisions within lineage B probably took place ~115 kya (Fig. 4; Tab. 3), in good agreement with our previously published data (Petrova *et al.*, 2015). There is a difference in the topology of basal splits between the dated tree (Fig. 4) and the tree without dating (Fig. 2). Cluster B1 either situates at the base of lineage B or is grouped with the rest of the western clusters (B2–B4) with low support. Relationships among clusters B2–B4 also proved to be unresolved (Fig. 4). Therefore, such a topology should be interpreted as polytomy at the base of lineage B.

Species distribution modelling

According to the results of the species distribution modelling (Fig. 5A–C), the proposed distribution of habitats suitable for *L. gregalis* lineage B is almost continuous both in cold (LGM) and warm (LIG and present) epochs. The optimal habitats in the LIG (Fig. 5C) were concentrated in South Siberia including the Altai-Sayan region, the Selenga River basin, the western slope of the Greater Khingan and even steppes north of the Sayan Mountains. During the LGM (Fig. 5B), suitable biotopes moved eastwards: the patch north of the Sayan Mountains disappeared, and the territory of eastern Tuva and bordering Mongolia (Yenisey River headwaters) also became unsuitable, while Selenga and the western slope of the Greater Khingan retained highly suitable habitats. A big suitable area appeared in the middle Amur River basin.

Table 3. Time estimates (ya: years ago) for some splitting events on the basis of cytochrome *b* data.

Nodes	Mean (ya)	95% HPD (ya)
<i>L. gregalis</i> — <i>L. raddei</i>	651 946	1 020 359–305 064
<i>L. gregalis</i> A — (B+C)	346 219	170 353–528 704
<i>L. gregalis</i> B — <i>L. gregalis</i> C	259 384	414 778–112 042
<i>L. gregalis</i> B MRCA	114 613	186 066–51 393
B1 MRCA. Southeastern Tuva, western Mongolia	28 936	51 278–9 557
B2 MRCA. Southeastern Tuva, Tannu-Ola	15 751	31 556–3 923
B3 MRCA. Lake Khuvsgul	12 138	26 697–1 608
B4 MRCA. Central Mongolia	5 856	16 326–69
B5 MRCA. Transbaikalia	33 134	55 510–14 083
B6 MRCA. Eastern Mongolia	21 559	36 028–8 505
B7 MRCA. Amur	23 174	45 832–6 327

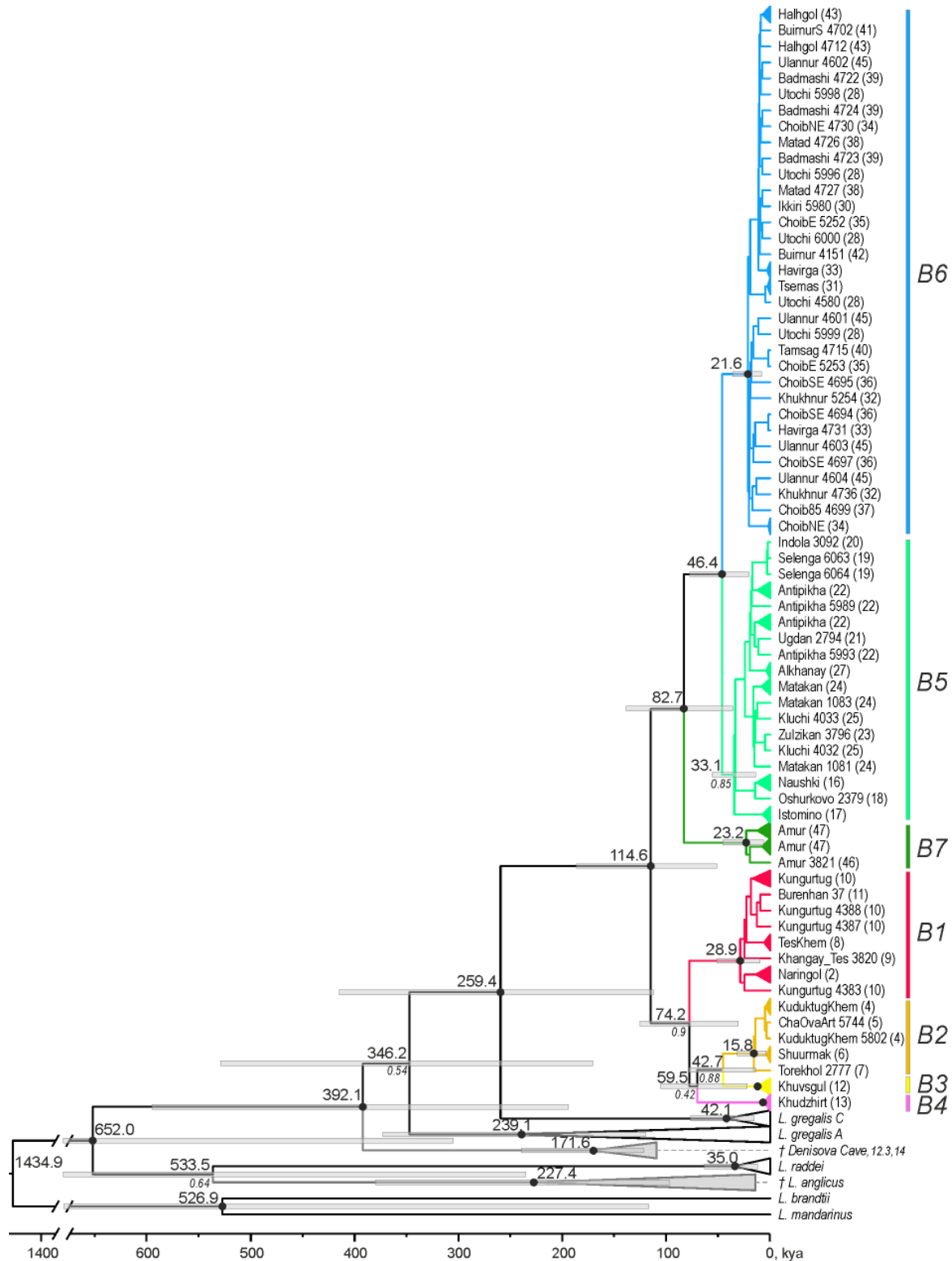


Fig. 4. The maximum clade credibility tree for narrow-headed vole cytochrome *b* haplotypes. Bayesian posterior probability (above 0.7) of major clades is presented as italic text below nodes; nodes with $bpp > 0.95$ are labelled with black circles. Mean node height in thousands of years ago (kya) is presented above nodes; node bars show 95% highest posterior density (HPD) intervals of node heights. For haplotype codes and location ID numbers (in brackets), refer to Fig. 1 and Appendix 1. For cluster names, refer to Fig. 3B. Outgroup taxa (*Alexandromys kikuchii*, *Neodon fuscus* and *Chionomys nivalis*) are not shown for better presentation.

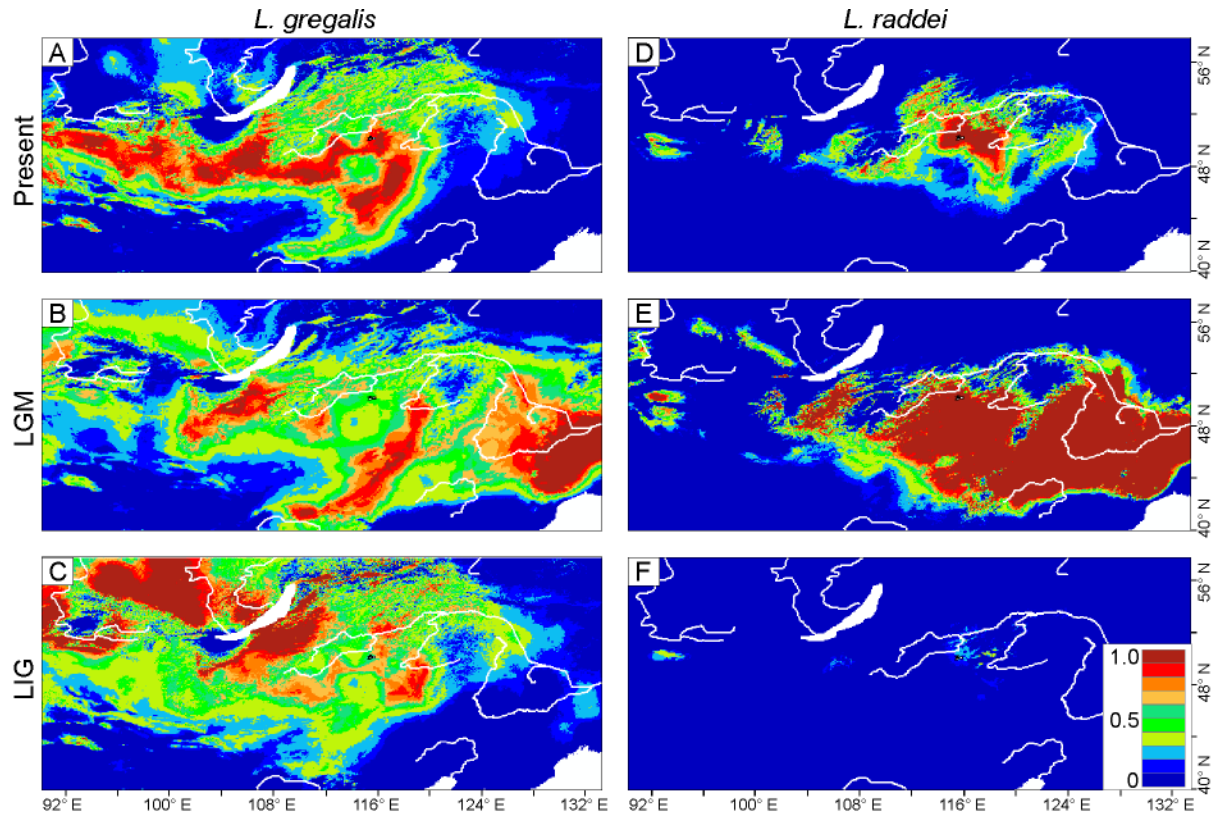


Fig. 5. The scheme of the proposed current and past distributions of habitats suitable for *Lasiopodomys gregalis* lineage B (A–C) and *L. raddei* (D–F). Models age given for the present (A and D), the last glacial maximum (LGM, B and E) and the last interglacial (LIG, C and F). Colours denote habitat suitability levels ranging from 0.0 (unsuitable) to 1.0 (best habitats) on a cloglog scale.

For *L. raddei*, conditions during the LIG were extremely unfavourable (Fig. 5F). By contrast, its suitable habitats in the LGM (Fig. 5E) extended across the steppes of the whole upper Amur River basin and an adjacent area of the basin of internal drainage, spreading much wider than nowadays (Fig. 5D). The Selenga River basin contained suitable habitats as well.

Discussion

Early divergences of narrow-headed voles

Being the most abundant species in all habitats throughout the Palearctic in the Late Pleistocene and hence often used for stratigraphic calibrations, the narrow-headed vole is a useful model for climatic and landscape reconstructions. A divergence dating analysis within major lineages of narrow-headed voles was performed some time ago (Petrova *et al.*, 2015), but molecular data on a number of Pleistocene tissue samples were obtained recently (Baca *et al.*, 2023), which allowed us to take advantage of the new reliable calibrations.

According to the results of the analysis based on *cytb* sequences, the time points of the main splits among narrow-headed voles match the ones we calcu-

lated earlier (Petrova *et al.*, 2015) and are notably older than those determined by Baca *et al.* (2023). This discrepancy apparently is due to the fact that the latter authors used only the tip dates as calibrations without taking into account the age of basal splits. This approach depreciates the relaxed clock algorithm and does not allow to trace a reduction in the observed evolution rates back in time (Ho *et al.*, 2005; Peterson & Masel, 2009). For instance, the biggest difference between the results of Baca *et al.* (2023) and our estimates is seen in deeper nodes, such as the separation of *L. gregalis* from *L. raddei* [178 kya with 95% highest posterior density (HPD): 210–148 kya (Baca *et al.*, 2023) versus 652 kya with 95% HPD 1020–305 kya] or the basal split within *L. gregalis* estimated at ~95 kya (Baca *et al.*, 2023; Fig. S3) versus our estimate of ~346 kya (Fig. 4; Tab. 3).

The dates we obtained for the main nodes among narrow-headed voles, despite being deeper than those published by Baca *et al.* (2023), are very low for the formation of full-rank species. Lineages A, B and C live allopatrically in the Altai-Sayan region and are well isolated from each other genetically; consequently, they can be recognised as separate taxa, probably of the lowest taxonomic rank (Petrova *et al.*, 2021). According to our estimates, the time of the basal split within

L. gregalis (A / B+C) is 170–529 kya (Tab. 3) with the mean value of 346 kya, as noted above.

Lasiopodomys gregalis lineage B geographic distribution

As we already stated, three lineages of *L. gregalis* (A, B and C) can come into contact in the Altai-Sayan region but remain genetically and spatially isolated (Petrova *et al.*, 2021). A single case of sympatry of *L. gregalis* genetic lineages B and C in central Tuva (Tuva Basin) confused us (Petrova *et al.*, 2015; 2021). According to the results of our new molecular analysis of the museum voucher specimens, we are forced to admit that this was a mistake. The confusion was caused by a mislabelled tissue sample. Thus, lineages B and C are entirely allopatric, and a geographic barrier is formed by forested northern slopes of the East Tannu-Ola Mountain Range, with the only possible contact zone being the corridor of suitable habitats along the mountain pass discussed by Petrova *et al.* (2021). The new data on mt *cytb* clarify the current position of the possible boundary between the lineages; at present, it possibly goes to the north from the Shuurmak Village inhabited by lineage B representatives (Fig. 1, loc. 6), whereas at ~40 km north of Shuurmak, lineage C was detected.

Representatives of lineage B also may come into contact with lineage A individuals in the vicinity of Lake Uvs-Nuur; however, no traces of sympatry or hybridisation were found. From the new analysed data, we can conclude that the northern boundary of the lineage B geographic range in Cisbaikalia is determined by southern slopes of the forested East Sayan Mountains and Khamar-Daban Mountain Range. According to the SDM results (Fig. 5A–C), unsuitable biotopes existed there during all the time periods analysed by us. In Transbaikalia, the northern border apparently is formed by the southern limit of the solid taiga zone from northern Baikal to the Amur River.

The contact zone of *L. gregalis* lineage B with *L. raddei* in Transbaikalia was discussed in detail in our earlier study (Petrova *et al.*, 2023). Although results of a microsatellite loci analysis there revealed traces of hybridisation, we did not find any populations where the species lived sympatrically; also no traces of hybridisation and subsequent introgression were detected by the analysis of mt *cytb* and of the nuclear *BRCA1* gene. Consequently, the new data clearly indicate that *L. gregalis* lineage B, despite the possibility of contact with *L. raddei* and lineages A and C of *L. gregalis*, does not mix with them throughout the geographic range from western Mongolia and southeastern Tuva to the Tunka basin, eastern Transbaikalia and the middle Amur River.

Until now, it has seemed that unlike *L. gregalis* lineage A (whose geographic range is highly fragmented), lineage B inhabits a territory devoid of obvious geographical barriers. Nevertheless, our findings unambiguously show that even on the territory of continuous suitable habitats throughout the entire modern geographic range (Fig. 5A), mitochondrial clusters within lineage B do not mix either (Fig. 3B). The only case

where it is impossible to suppose a clear-cut boundary between the groupings is clusters B1 and B2 in western Mongolia and southeastern Tuva.

Lasiopodomys gregalis lineage B evolutionary history

Phylogenetic reconstruction in MrBayes (Fig. 2) revealed a sister position of cluster B1 towards all other clusters, B2–B7, albeit with moderate support. The topology of the dated tree (Fig. 4) slightly differs and does not show the basal position of the B1 cluster. Nevertheless, because the territory to the north of the Eastern Tannu-Ola Mountain Range (the basin of upper reaches of the Yenisey River) is inhabited by *L. gregalis* lineage C (Petrova *et al.*, 2021), which is sister to lineage B, it can be theorised that the area of origin and accordingly the source of the spread of lineage B was located on a neighbouring territory.

On the basis of the divergence dates (Fig. 4) and the dynamics of suitable habitats (Fig. 5), we can advance a hypothesis about the formation of the modern geographic range of *L. gregalis* lineage B. Probably at the end of the LIG or after it, ~115 kya according to divergence dating (Fig. 4), the geographic range of *L. gregalis*, except for lineages A and C's geographic ranges (Fig. 6C, to the southeast of the black dotted line), was clearly divided into two parts: western and eastern. Representatives of the modern B1 cluster inhabiting western Mongolia and southeastern Tuva may be descendants of the western group. Although this territory was less suitable for *L. gregalis* during cold epochs (Fig. 5B), cluster B1 is characterised by high nucleotide diversity (Tab. 2), indicating the absence of sharp fluctuations in the population size.

It is unclear exactly how the eastern part of the geographic range was occupied (Fig. 6C); in the LIG, almost all the territory of northern Mongolia was suitable enough (Fig. 5C), but in the subsequent cold period — probably the Ermakov (=early Zyryan) glacial period, which took place ~75–50 kya — a band of unsuitable biotopes could emerge to the west and south of Lake Khuvsgul, as proposed for the LGM (Fig. 5B), thereby separating the Selenga River basin from the westernmost regions.

During cold epochs (as proposed for the LGM, Fig. 5E), favourable conditions for the dispersion of *L. raddei* could form. We assume that the increase of *L. raddei*'s geographic range led to the displacement of *L. gregalis* from suitable habitats, and thereby the eastern part of its geographic range was fragmented, with the separation of clusters B4, B5 and B7 (Fig. 6B). Divergence dates (Fig. 4) suggest that this separation took place before the LGM. The displacement of *L. gregalis* by *L. raddei* is indirectly confirmed by the absence of ancestral polymorphism in modern *L. gregalis* populations in eastern Mongolia.

The separation of the B6 cluster (the settlement in eastern Mongolia) can be considered a relatively recent event. These populations are probably a derivative of the populations of Transbaikalia (B5) because the former occupy a terminal position on the haplotype network

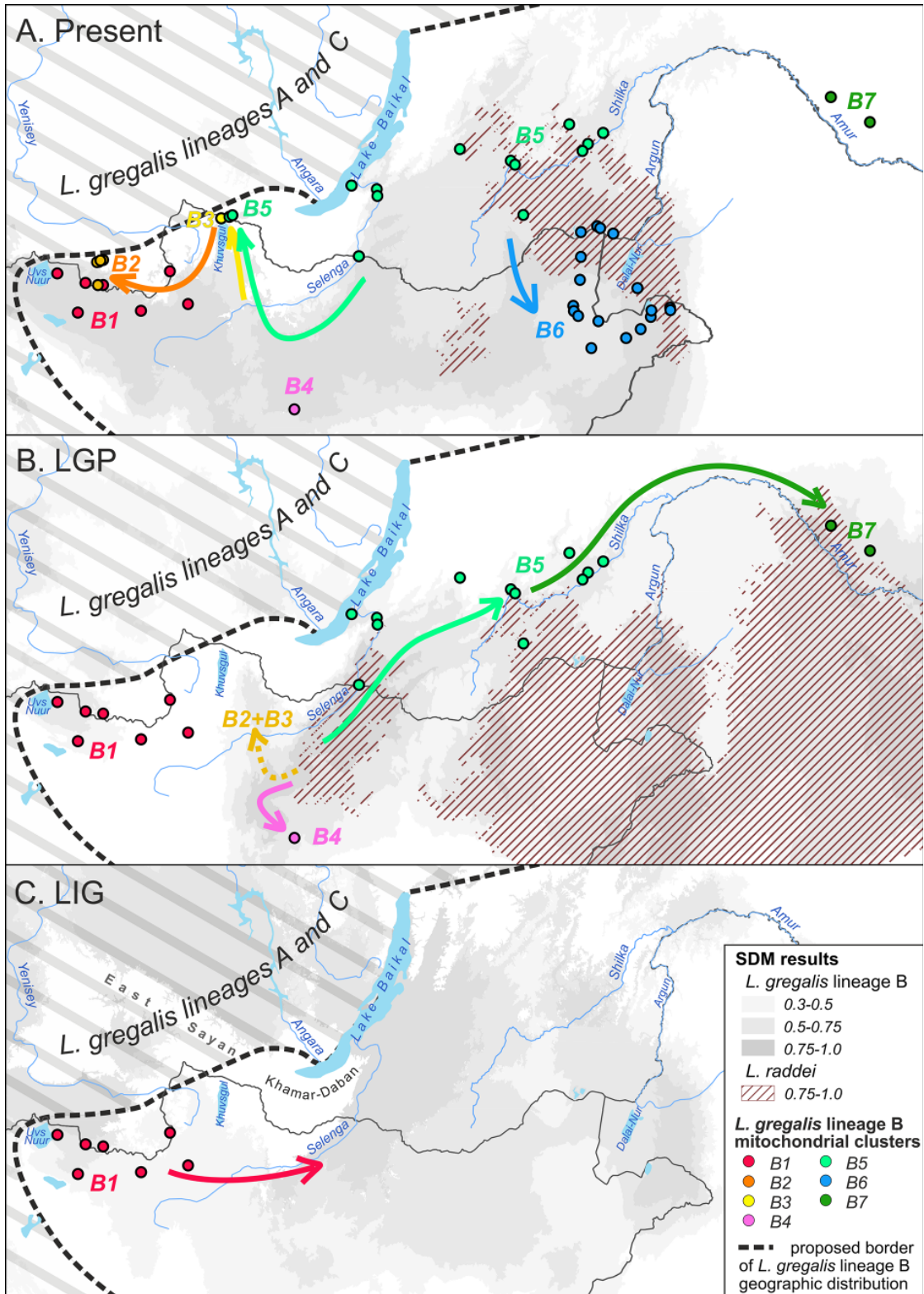


Fig. 6. The proposed scheme of formation of the modern geographic range of *Lasiopodomys gregalis* lineage B. A: The present; B: the last glacial period (LGP); C: the last interglacial (LIG). The proposed border of the *L. gregalis* lineage B geographic range is the bold dotted line; lineages A and C's geographic range is indicated by wide hatching. For *L. gregalis*, habitat suitability intervals on a cloglog scale are marked with a solid fill, with a darker colour meaning higher suitability. For *L. raddei*, only the highest suitability range is shown (marked with narrow hatching); for a complete scheme, see Fig. 5D–F. Sampling localities and the positions of rivers and lakes are modern.

(Fig. 3A). Currently, Transbaikalia and eastern Mongolian clusters are geographically separated by the territory occupied by *L. raddei* (Petrova *et al.*, 2023). According to the SDM results, we can suppose that in contrast to the prosperity during cold epochs (Fig. 5E), *L. raddei* underwent a reduction in the geographic range and a corresponding demographic decline during interglacials (Fig. 5D, F); consequently, perhaps up to the LGM, eastern Mongolia could be periodically inhabited by *L. raddei*. Representatives of *L. gregalis* probably broke through *L. raddei* to eastern Mongolia after the LGM (Fig. 6A), when *L. raddei* population density decreased. As reported by Petrova *et al.* (2015; Fig. 4), *L. raddei* (haplogroup 'D') demonstrates starlike structure on the haplotype network. The dispersal was probably carried out by a small number of *L. gregalis* founders because populations of eastern Mongolia (B6 cluster) exhibited a founder (or probably a bottleneck) effect: starlike structure on the haplotype network (Fig. 3A) and low indices of genetic diversity (Tab. 2).

Apparently, judging by the modelling results, the separation of the B3+B2 ancestors' branch also occurred in a cold epoch (Fig. 6B), although their modern range was not suitable during the Ice Age. Therefore, this group could probably inhabit territory to the east of Lake Khuvsgul.

Possibly, after the LGM, the western and eastern parts of the *L. gregalis* lineage B geographic range merged (Fig. 6A). At the same time, representatives of the Transbaikalia B5 cluster returned to the west of Lake Baikal and are nowadays found in the Tunka basin. Clusters B2 and B3 (probably inhabiting the territory east of Khuvsgul Lake) were also able to spread to the west, and currently, representatives of clusters B3 and B5 inhabit neighbouring territories to the north of Lake Khuvsgul, while cluster B2 representatives almost mixed with descendants of ancestral lineage B1 in western Mongolia and southeastern Tuva (Fig. 6A). Nevertheless, we did not find any sympatric localities of clusters B1 and B2 even on the seemingly homogeneous territory of the Ubsunur basin. It is difficult to explain this pattern, which replicates the situation observed in narrow-headed voles at higher taxonomic levels, e.g. the absence of sympatric populations of cryptic species *L. raddei* and *L. gregalis* in Transbaikalia (Petrova *et al.*, 2023) and the allopatry of lineages A, B and C within *L. gregalis* in the Altai-Sayan Region (Petrova *et al.*, 2021). In the absence of geographical barriers, the genetic isolation could be explained by some behavioural features or post-zygotic isolation mechanisms, but there are no such data yet. To investigate population processes at different taxonomic levels, an analysis of single-nucleotide polymorphisms from genomic data is needed.

Comparative phylogeography of steppe mammals

Several steppe species inhabiting Mongolia and adjacent territories are similar in phylogeographic structure to the narrow-headed vole; therefore, it is interest-

ing to compare these patterns for gaining a more complete understanding of the history of steppe landscapes of Southern Siberia.

One of the species highly similar to narrow-headed voles both in ecology and in the structure of the geographic range is *Cricetulus barabensis* Pallas, 1773. The geographic range of the two main 20-chromosome sublineages (*C. b. barabensis* + *C. b. tuvinicus* and *C. b. xinganensis* + *C. b. ssp*) is similar to the *L. gregalis* lineage B range. Poplavskaya *et al.* (2019) hypothesised that during the Kazantsevo interglacial (130–110 kya), these sublineages were restricted to disjoint refugial areas (probably located in central Mongolia/west Transbaikalia and the Amur region) owing to interglacial expansion of forests in the Hentei–Khangai area (Golubeva, 1978). Centres of diversity of these *C. barabensis* lineages are highly similar to the ones predicted for *L. gregalis* lineage B, but during a comparison of divergence times of these groups, notable rate discrepancies were revealed. For instance, according to our results, the time of the split between lineages B and C of *L. gregalis* is estimated as 259.4 kya (95% HPD: 415–112), well consistently with the basal radiation time of *C. barabensis* *sensu lato* into three lineages: 262 kya (95% HPD: 610–159), although *p*-distances in these groups differ almost twofold. Within three groups of *C. barabensis* *s.l.*, *p*-distances are 2.3–4.2%, whereas between lineages B and C of *L. gregalis*, they are 6.2%. Perhaps this finding is explained by a high *cytb* mutation rate in voles in general and in narrow-headed voles in particular. A disproportionate increase in the mutation rate at the ends of the branches does not allow us to conduct the divergence dating analysis correctly.

Another wide-ranging steppe dweller is the long-tailed ground squirrel *Urocitellus undulatus* Pallas, 1778. *U. u. evermanni* demonstrates high variation in western Mongolia, whereas individuals from Uvs Aimag (Ubsunur basin) in particular have been detected in different lineages (McLean *et al.*, 2018), in good agreement with the pattern observed for *L. gregalis*, which demonstrates a mixture of clusters B1 and B2 on this territory.

Floral biodiversity in general and steppe biocoenoses in particular are among the richest ones in the Altai-Sayano-Baikal mountain country. Large numbers of both endemic and relict species have been found in extra-zonal mountain-steppe complexes of the forest-steppe belt of South Siberia; accordingly, one can suppose that these habitats serve as refugia (Kyrgys *et al.*, 2009; Namzalov, 2009; Namzalov, 2020). Three major nodes of floral biodiversity have been detected: Sailugem-Mongun-Taiginsky in the Altai and western Tuva, Sangilensko-Darkhatsky in southeastern Tuva and Mongolia and Selenginsko-Daursky in Transbaikalia (Namzalov, 2021). It is curious that their location clearly coincides with the diversity centres of narrow-headed voles. The Altai is a centre of the geographic range of *L. gregalis* lineage A (Petrova *et al.*, 2015). In southeastern Tuva, we assume separation of an *L. gregalis* ancestral group into three lineages: A, B and C (Petrova *et al.*, 2021). In Transbaikalia, the cryp-

tic species *L. raddei* — apparently a relic of the early Pleistocene — was found (Petrova *et al.*, 2016), and this territory is also a probable centre of dispersal of clusters B2–B7 of *L. gregalis* lineage B. As described above, these territories are also centres of diversity of other steppe dwellers. Thus, in the context of steppe landscapes' history, the phylogeographic data on *L. gregalis* in the southern part of its geographic range match well the hypothesis advanced by Poplavskaya *et al.* (2019). This hypothesis combines data on several steppe dwellers and indicates the existence of two major refugia in Mongolian steppe in the past: in the vicinities of Sangilen Uplands and in Transbaikalia in the Selenga River basin.

Conclusions

For lineage B of *L. gregalis*, despite the absence of visible geographical barriers, well-pronounced phylogeographic structure was uncovered. The source of the spread of this lineage at the end of the LIG was probably the territory of western Mongolia and south-eastern Tuva. Mitochondrial clusters within this lineage turned out to be almost allopatric, thereby replicating the pattern seen in narrow-headed voles at higher taxonomic levels. Apparently, the modern structure of the *L. gregalis* geographic range in Mongolia and surrounding territories has formed as a result of i) competitive interactions with the cryptic species *L. raddei* and ii) climatic fluctuations.

ACKNOWLEDGEMENTS. We express our deep gratitude to Natalia I. Abramson, under whose leadership this project began. We are grateful to colleagues from the Tuvian Institute for Exploration of Natural Resources SB RAS, Kyzyl (Valentin V. Zaika, Svetlana V. Kuzhuget, Vyacheslav A. Kyzyl-ool and Aleksander D. Saaya) for help with the organisation of the field studies, Aivar V. Kuular (Tuvan State University, Kyzyl), Georgy B. Ryurikov (A.N. Severtsov Institute of Ecology and Evolution, RAS, Moscow), Sergey A. Abramov and Igor V. Moroldoev (Institute of Systematics and Ecology of Animals, SB RAS, Novosibirsk), who helped with the collecting of the material. The field work was carried out with partial support from grant No. FWGS-2021-0002 (to Natalia V. Lopatina). We thank Tamara A. Sirokhina (Irkutsk State University) and Vladimir S. Lebedev (Zoological Museum, Moscow State University), who allowed us to analyse tissue samples from the museum collections. The authors are also grateful to Alexey S. Tesakov for the discussion of the material from Denisova Cave. The laboratory work was done on the equipment of the Taxon research resource center (<http://www.ckp-rf.ru/ckp/3038/>) of the Zoological Institute RAS (St. Petersburg). Besides, we are thankful to two anonymous reviewers for their helpful critical comments. The English language was corrected by shevchuk-editing.com. This research was funded by the Russian Science Foundation (RSF), grant No. 22-24-00513, <https://rscf.ru/project/22-24-00513/>.

References

- Abramson N.I., Rodchenkova E.N. & Kostygov A.Yu. 2009. Genetic variation and phylogeography of the bank vole (*Clethrionomys glareolus*, Arvicolinae, Rodentia) in Russia with special reference to the introgression of the mtDNA of a closely related species, red-backed vole (*Cl. rutilus*) // Russian Journal of Genetics. Vol.45. No.5. P.533–545.
- Baca M., Popović D., Agadzhanian A.K., Baca K., Conard N.J., Fewlass H., Filek T., Golubiński M., Horáček I., Knul M.V., Krajcarz M., Krokhalova M., Lebreton L., Lemanik A., Maul L.C., Nagel D., Noiret P., Primault J., Rekovets L., Rhodes S.E., Royer A., Serdyuk N.V., Soressi M., Stewart J.R., Strukova T., Talamo S., Wilczyński J. & Nadachowski A. 2023. Ancient DNA of narrow-headed vole reveal common features of the Late Pleistocene population dynamics in cold-adapted small mammals // Proceedings of the Royal Society B: Biological Sciences. Vol.290. P.20222238.
- Baca M., Popović D., Lemanik A., Baca K., Horáček I. & Nadachowski A. 2019. Highly divergent lineage of narrow-headed vole from the Late Pleistocene Europe // Scientific Reports. Vol.9. No.1. P.17799.
- Bannikova A.A., Lebedev V.S., Lisovsky A.A., Matrosova V., Abramson N.I., Obolenskaya E.V. & Tesakov A.S. 2010. Molecular phylogeny and evolution of the Asian lineage of vole genus *Microtus* (Rodentia: Arvicolinae) inferred from mitochondrial cytochrome *b* sequence // Biological Journal of the Linnean Society. Vol.99. No.3. P.595–613.
- Bouckaert R., Heled J., Kühnert D., Vaughan T., Wu C.-H., Xie D., Suchard M.A., Rambaut A. & Drummond A.J. 2014. BEAST 2: a software platform for Bayesian evolutionary analysis // PLoS Computational Biology. Vol.10. No.4. P.e1003537.
- Fick S.E. & Hijmans R.J. 2017. WorldClim 2: new 1-km spatial resolution climate surfaces for global land areas // International Journal of Climatology. Vol.37. No.2. P.4302–4315.
- Gerasimov I.P. & Velichko A.A. 1982. [Paleogeography of Europe during the last 100,000 years (Atlas-Monograph)]. Moscow: Nauka. 175 p. [in Russian].
- Golubeva L.V. 1978. [Vegetation of Northern Mongolia in the Pleistocene and Holocene (the Selenga and Orkhon River basins)] // Izvestiya Akademii nauk SSSR, Seriya Geologicheskaya. Vol.3. P.68–81 [in Russian].
- Hall T.A. 1999. BioEdit: a user-friendly biological sequence alignment editor and analysis program for Windows 95/98/NT // Nucleic Acids Symposium Series. Vol.41. P.95–98.
- Ho S.Y., Phillips M.J., Cooper A. & Drummond A.J. 2005. Time dependency of molecular rate estimates and systematic overestimation of recent divergence times // Molecular biology and evolution. Vol.22. No.7. P.1561–1568.
- Hoang D.T., Chernomor O., Von Haeseler A., Minh B.Q. & Vinh L.S. 2018. UFBoot2: improving the ultrafast bootstrap approximation // Molecular Biology and Evolution. Vol.35. No.2. P.518–522.
- Karamysheva Z.V. 1988. [Latitudinal and longitudinal changes in the montane vegetation of Mongolia // Flora of high-mountain ecosystems of the USSR]. Vladivostok: DVO AN SSSR. P.262–273 [in Russian].
- Karger D., Conrad O., Böhner J., Kawohl T., Kreft H., Soria-Auza R.W., Zimmermann N.E., Linder H.P. & Kessler M. 2017. Climatologies at high resolution for the earth's land surface areas // Scientific Data. Vol.4. P.170122.

- Kass J.M., Muscarella R., Galante P.J., Bohl C.L., Pinilla-Buitrago G.E., Boria R.A., Soley-Guardia M., Anderson R.P. 2021. ENMeval 2.0: Redesigned for customizable and reproducible modeling of species' niches and distributions // *Methods in Ecology and Evolution*. Vol.12. P.1602–1608.
- Kowalski K. 2001. Pleistocene rodents of Europe // *Folia Quaternaria*. Vol.72. P.3–389.
- Kumar S., Stecher G. & Tamura K. 2016. MEGA7: molecular evolutionary genetics analysis version 7.0 for bigger datasets // *Molecular Biology and Evolution*. Vol.33. No.7. P.1870–1874.
- Kyrgys K.V., Namzalov B.B. & Dubrovskii N.G. 2009. [Steppes of Sangilen Plateau (Southeastern Tyva)]. Kyzyl: Tyvinskoe Knizhnoye Izdatelstvo. 160 p. [in Russian].
- Lanfear R., Frandsen P.B., Wright A.M., Senfeld T. & Calcott B. 2016. PartitionFinder 2: new methods for selecting partitioned models of evolution for molecular and morphological phylogenetic analyses // *Molecular Biology and Evolution*. P.msw260.
- Makunina N.I., Maltseva T.V. & Parshutina L.P. 2007. [The mountain forest-steppe of Tuva] // *Vegetation of Russia*. No.10. P.61–88 [in Russian].
- Markova A. & Van Kolfshoten T. 2008. Evolution of the European ecosystems during Pleistocene-Holocene transition (24–8 kyr BP). Moscow: KMK Scientific Press. 556 p.
- Martin R.A., Peláez-Campomanes P., Honey J.G., Fox D.L., Zakrzewski R.J., Albright L.B., Lindsay E.H., Opdyke N.D. & Goodwin H.T. 2008. Rodent community change at the Pliocene–Pleistocene transition in southwestern Kansas and identification of the *Microtus* immigration event on the Central Great Plains // *Palaeogeography, Palaeoclimatology, Palaeoecology*. Vol.267. No.3–4. P.196–207.
- McLean B.S., Batsaikhan N., Tchabovsky A. & Cook J.A. 2018. Impacts of late Quaternary environmental change on the long-tailed ground squirrel (*Urocitellus undulatus*) in Mongolia // *Zoological Research*. Vol.39. No.5. P.364–372.
- Muscarella R., Galante P.J., Soley-Guardia M., Boria R.A., Kass J.M., Uriarte M. & Anderson R.P. 2014. ENMeval: An R package for conducting spatially independent evaluations and estimating optimal model complexity for Maxent ecological niche models // *Methods in Ecology and Evolution*. Vol.5. P.1198–1205.
- Namzalov B.B. 2009. Baikal phytogeographic node as the newest center of endemism of Inner Asia // *Contemporary Problems of Ecology*. Vol.2. No.4. P.340–346.
- Namzalov B.B. 2020. Extrazonal steppe phenomena in the mountains of Southern Siberia: features of spatial organization and centers of the latest speciation and cenogenesis // *Contemporary Problems of Ecology*. Vol.13. No.5. P.495–504.
- Namzalov B.B. 2021. [The most important nodes of biodiversity and phytogeographic phenomena of mountain steppes of Southern Siberia] // *Arid ecosystems*. Vol.27. No.3. P.24–36 [in Russian].
- Peterson G.I. & Masel J. 2009. Quantitative prediction of molecular clock and ka/ks at short timescales // *Molecular Biology and Evolution*. Vol.26. No.11. P.2595–2603.
- Petrova T.V. 2017. [Narrow-headed vole *Lasiopodomys (Stenocranius) gregalis* (Pallas, 1779): taxonomic structure, phylogenetic position and evolution]. Saint Petersburg: Zoological Institute RAS. 141 p. [in Russian].
- Petrova T.V., Dvoyashov I.A., Bazhenov Y.A., Obolenskaya E.V. & Lissovsky A.A. 2023. An invisible boundary between geographic ranges of cryptic species of narrow-headed voles (*Stenocranius, Lasiopodomys*, Cricetidae) in Transbaikalia // *Diversity*. Vol.15. No.3. P.439.
- Petrova T.V., Genelt-Yanovskiy E.A., Lissovsky A.A., Chash U.-M.G., Masharsky A.E. & Abramson N.I. 2021. Signatures of genetic isolation of the three lineages of the narrow-headed vole *Lasiopodomys gregalis* (Cricetidae, Rodentia) in a mosaic steppe landscape of South Siberia // *Mammalian Biology*. Vol.101. No.3. P.275–285.
- Petrova T.V., Tesakov A.S., Kowalskaya Y.M. & Abramson N.I. 2016. Cryptic speciation in the narrow-headed vole *Lasiopodomys (Stenocranius) gregalis* (Rodentia: Cricetidae) // *Zoologica Scripta*. Vol.45. No.6. P.618–629.
- Petrova T.V., Zakharov E.S., Samiya R. & Abramson N.I. 2015. Phylogeography of the narrow-headed vole *Lasiopodomys (Stenocranius) gregalis* (Cricetidae, Rodentia) inferred from mitochondrial cytochrome *b* sequences: an echo of Pleistocene prosperity // *Journal of Zoological Systematics and Evolutionary Research*. Vol.53. No.2. P.97–108.
- Poplavskaya N., Bannikova A., Neumann K., Pavlenko M., Kartavtseva I., Bazhenov Y., Bogomolov P., Abramov A., Surov A. & Lebedev V. 2019. Phylogeographic structure in the chromosomally polymorphic rodent *Cricetulus barabensis* sensu lato (Mammalia, Cricetidae) // *Journal of Zoological Systematics and Evolutionary Research*. Vol.57. No.3. P.679–694.
- Prost S., Guralnick R.P., Waltari E., Fedorov V.B., Kuzmina E., Smirnov N., Van Kolfshoten T., Hofreiter M. & Vrieling K. 2013. Losing ground: past history and future fate of Arctic small mammals in a changing climate // *Global Change Biology*. Vol.19. No.6. P.1854–1864.
- Rambaut A., Drummond A.J., Xie D., Baele G. & Suchard M.A. 2018. Posterior summarization in bayesian phylogenetics using Tracer 1.7 // *Systematic Biology*. Vol.67. No.5. P.901–904.
- Ronquist F., Teslenko M., Van der Mark P., Ayres D.L., Darling A., Höhna S., Larget B., Liu L., Suchard M.A. & Huelsenbeck J.P. 2012. MrBayes 3.2: efficient Bayesian phylogenetic inference and model choice across a large model space // *Systematic Biology*. Vol.61. No.3. P.539–542.
- Rozas J., Ferrer-Mata A., Sánchez-DelBarrio J.C., Guirao-Rico S., Librado P., Ramos-Onsins S.E. & Sánchez-Gracia A. 2017. DnaSP 6: DNA sequence polymorphism analysis of large data sets // *Molecular Biology and Evolution*. Vol.34. No.12. P.3299–3302.
- Tesakov A.S., Vangengeim E.A. & Pevzner M.A. 1999. Findings of the oldest rootless voles *Allophaiomys* and *Prolagurus* in Eastern Europe // *Doklady of the Russian Academy of Sciences / Earth Science Section* : Vol.366. P.452.
- Thompson J.D., Higgins D.G. & Gibson T.J. 1994. CLUSTAL W: improving the sensitivity of progressive multiple sequence alignment through sequence weighting, position-specific gap penalties and weight matrix choice // *Nucleic Acids Research*. Vol.22. No.22. P.4673–4680.
- Trifinopoulos J., Nguyen L.-T., Von Haeseler A. & Minh B.Q. 2016. W-IQ-TREE: a fast online phylogenetic tool for maximum likelihood analysis // *Nucleic Acids Research*. Vol.44. No.W1. P.W232–W235.
- Zheng S. & Zhang Z. 2001. Late Miocene–Early Pleistocene micromammals from Wenwanggou of Lingtai, Gansu, China // *Vertebrata Palasiatica*. Vol.38. No.1. P.58–71.

Appendix 1. Material used in the genetic analysis. Museum voucher abbreviations: ZMMU, Zoological Museum Moscow State University; ZIN, Zoological Institute RAS; IBSS, Institute of Biology and Soil Science FEB RAS; ISEA, Institute of Systematics and Ecology of Animals SB RAS; and ISU, Irkutsk State University. Tissue samples from the museum collections are marked with an asterisk. Sequences obtained in the current study are highlighted in bold, and those taken from previous studies are indicated by superscripted numbers: ¹from Petrova *et al.* (2021); ²from Petrova *et al.* (2015); ³from Lissovsky *et al.* (2013); ⁴from Petrova *et al.* (2016); and ⁵from Petrova *et al.* (2023).

Map ID	Locality, coordinates	Tissue ID	Tree code	Mt cluster	Museum voucher	GenBank acc. No.
1	Russia, Tuva, Uvsnuur Lake, Naringol River, 50.337°N, 93.396°E	4780	Uvsnuur	B1	ZMMU s-52426*	OR004258
2	Russia, Tuva, Erzinsky District, Narin-Gol, 50.104°N, 94.596°E	4910	Naringol	B1	ZIN 105693	MT119799 ¹
		4912	Naringol	B1	ZIN 105696	MT119800 ¹
		4913	Naringol	B1	ZIN 105697	MT119801 ¹
		4914	Naringol	B1	ZIN 105702	MT119802 ¹
		4915	Naringol	B1	ZIN 105704	MT119803 ¹
3	Mongolia, Hanhuhei Range, Khulan, 49.366°N, 94.273°E	4778	Hanhuhei	B1	ZMMU s-42092*	OR004259
4	Russia, Tuva, Tes-Khemsy District, NE from Samagaltay, Kuduktug-Khem River, 50.623°N, 95.083°E	5800	KuduktugKhem	B2	ZIN 107056	OR004260
		5801	KuduktugKhem	B2	ZIN 107057	OR004261
		5802	KuduktugKhem	B2	ZIN 107058	OR004262
		5806	KuduktugKhem	B2	ZIN 107059	OR004263
5	Russia, Tuva, Tes-Khemsy District, Cha-Ova-Art, 50.63°N, 95.165°E	5744	ChaOvaArt	B2	ZIN 107055	OR004264
6	Russia, Tuva, Tes-Khemsy District, 3 km NE of Shuurmak, 50.674°N, 95.355°E	5741	Shuurmak	B2	ZIN 107052	OR004265
		5742	Shuurmak	B2	ZIN 107053	OR004266
		5891	Shuurmak	B2	ZMMU s-208502	OR004267
7	Russia, Tuva, Erzinsky District, Tore-Khol Lake, 50.051°N, 95.118°E	2777	Torekhol	B2	ZMMU s-188787*	KJ192307 ²
8	Russia, Tuva, Erzinsky District, Tes-Khem River, 50.055°N, 95.35°E	5892	TesKhem	B1	ZMMU s-208503	OR004268
		5893	TesKhem	B1	ZMMU s-208504	OR004269
		5894	TesKhem	B1	ZMMU s-208505	OR004270
		5895	TesKhem	B1	ZMMU s-208506	OR004271
		5896	TesKhem	B1	ZMMU s-208507	OR004272
		5897	TesKhem	B1	ZMMU s-208508	OR004273
9	Mongolia, Dzavhan District, Khangay, Tes, 49.40°N, 96.92°E	3820	Khangay_Tes	B1	ZIN 55985	KJ192296 ²
		4159	Khangay_Tes	B1	ZIN 55984	OR004275
10	Russia, Tuva, Tere-Kholsky District, 50 km SE from Kungurtug, 50.4°N, 98.2°E	4381	Kungurtug	B1	_	MT119804 ¹
		4383	Kungurtug	B1	_	MT119805 ¹
		4384	Kungurtug	B1	_	MT119806 ¹
		4385	Kungurtug	B1	_	MT119807 ¹
		4386	Kungurtug	B1	_	MT119808 ¹
		4387	Kungurtug	B1	_	MT119809 ¹
		4388	Kungurtug	B1	_	MT119810 ¹
4389	Kungurtug	B1	_	MT119811 ¹		
11	Mongolia, Khuvsgul District, Burenhan, 49.53°N, 98.9°E	37	Burenhan	B1	ZMMU S-179176	KJ192295 ²
12	Mongolia, Khuvsgul District, northern shore of Khuvsgul Lake, 51.617°N, 100.5°E	4608	Khuvsgul	B3	ISEA 61589	OR004276
		4609	Khuvsgul	B3	ISEA 61591	OR004277
		4610	Khuvsgul	B3	ISEA 61592	OR004278
		4611	Khuvsgul	B3	ISEA 61593	OR004279
		4612	Khuvsgul	B3	ISEA 61182	OR004280
13	Mongolia, Uverkhangay, 22 km SE Khudzhirt, 46.75°N, 102.97°E	4427	Khudzhirt	B4	ZMMU S-191064	OR004281
		4428	Khudzhirt	B4	ZMMU S-191065	OR004282
14	Russia, Buryatia, Tunkinsky District, 51.64°N, 100.87°E	6080	Tunka	B5	ISU 7024*	OR004285

Appendix 1. (*continuation*)

15	Russia, Buryatia, Tunkinsky District, Mondy, 51.68°N, 101.0°E	6081	Tunka	B5	ISU 7473*	OR004286
16	Russia, Buryatia, Kyakhtinsky District, Naushki, 50.37°N, 106.25°E	35	Naushki	B5	ZMMU S-179177	KF751098 ³
		36	Naushki	B5	ZMMU S-179178	KF751099 ³
17	Russia, Buryatia, Kabansky District, Istomino, 52.14°N, 106.32°E	2380	Istomino	B5	IBSS 2029	KF751101 ³
		2381	Istomino	B5	IBSS 2032	KF751102 ³
		2382	Istomino	B5	IBSS 2033	KF751103 ³
		2383	Istomino	B5	IBSS 2035	KF751104 ³
18	Russia, Buryatia, Ulan-Udinsky District, Oshurkovo, 51.96°N, 107.40°E	2379	Oshurkovo	B5	IBSS 1989	KF751100 ³
19	Russia, Buryatia, Ivolginsky District, Khojtobeye Village, 51.797°N, 107.395°E	6063	Selenga	B5	IBSS 62506	OR004283
		6064	Selenga	B5	IBSS 62507	OR004284
20	Russia, Buryatia, Yeravninsky District, Indola, 52.633°N, 111.3°E	3092	Indola	B5	-	KJ192306 ²
21	Russia, Zabaykalskiy Territory, Chita, Ugdan, 52.1°N, 113.4°E	2794	Ugdan	B5	-	KF751077 ³
22	Russia, Zabaykalskiy Territory, Chita, Antipikha, 51.988°N, 113.559°E	5988	Antipikha	B5	-	OP765436 ⁵
		5989	Antipikha	B5	-	OP765437 ⁵
		5990	Antipikha	B5	-	OP765438 ⁵
		5991	Antipikha	B5	-	OP765439 ⁵
		5992	Antipikha	B5	-	OP765440 ⁵
		5993	Antipikha	B5	-	OP765441 ⁵
		5994	Antipikha	B5	-	OP765442 ⁵
5995	Antipikha	B5	-	OP765443 ⁵		
23	Russia, Zabaykalskiy Territory, Nerchinskiy District, Zulzikan, 52.7°N, 116.3°E	3796	Zulzikan	B5	ZMMU S-23252	KJ192297 ²
24	Russia, Zabaykalskiy Territory, Sretenskiy District, Matakan, 52.27°N, 117.64°E	1081	Matakan	B5	ZMMU S-182032	KF751078 ³
		1083	Matakan	B5	ZMMU S-182034	KF751079 ³
		4034	Matakan	B5	ZIN 101669	KJ192298 ²
		4035	Matakan	B5	ZIN 101670	KJ192299 ²
		4036	Matakan	B5	ZIN 101674	KJ192300 ²
		4037	Matakan	B5	ZIN 101671	KJ192301 ²
		4038	Matakan	B5	ZIN 101672	KJ192302 ²
4039	Matakan	B5	ZIN 101673	KJ192303 ²		
25	Russia, Zabaykalskiy Territory, Nerchinskiy District, Nizhniye Kluchi, 52.096°N, 116.887°E	4032	Kluchi	B5	ZIN 101668	KJ192304 ²
		4033	Kluchi	B5	-	KJ192305 ²
26	Russia, Zabaykalskiy Territory, Nerchinskiy District, Nerchinsk, 51.9°N, 116.6°E	4250	Nerchinsk	B5	ZIN 6218	KT336549 ⁴
27	Russia, Zabaykalskiy Territory, Duldurginskiy District, Alkhanay 50.73°N, 113.48°E	4420	Alkhanay	B5	-	OP765434 ⁵
		4421	Alkhanay	B5	-	OP765435 ⁵
28	Russia, Zabaykalskiy Territory, Borzinskiy District, Utochi, 50.004°N, 115.720°E	4755	Utochi	B6	-	OP765477 ⁵
		4605	Utochi	B6	-	OP765478 ⁵
		4607	Utochi	B6	-	OP765479 ⁵
		4580	Utochi	B6	-	OP765480 ⁵
		5996	Utochi	B6	-	OP765481 ⁵
		5998	Utochi	B6	-	OP765482 ⁵
		5999	Utochi	B6	-	OP765483 ⁵
6000	Utochi	B6	-	OP765484 ⁵		

Appendix 1. (continuation)

29	Russia, Zabaykalskiy Territory, Borzinskiy District, 12 km NW Haranur Lake, 50.018°N, 116.507°E	4739	Haranur	B6	-	OP765485 ⁵
		4740	Haranur	B6	ZIN 105339	OP765486 ⁵
		4741	Haranur	B6	ZIN 105340	OP765487 ⁵
30	Russia, Zabaykalskiy Territory, Borzinskiy District, Ikkiri, 49.983°N, 116.550°E	5980	Ikkiri	B6	-	OP765488 ⁵
31	Russia, Zabaykalskiy Territory, Zabaikalskiy District, Tsemas, 49.767°N, 117.017°E	5977	Tsemas	B6	-	OP765489 ⁵
		5979	Tsemas	B6	-	OP765490 ⁵
32	Mongolia, Dornod, 9 km SW of Khukh-Nuur Lake, 49.401°N, 115.485°E	4736	Khukhnur	B6	ZIN 103855	OP765474 ⁵
		4737	Khukhnur	B6	ZIN 103856	OP765475 ⁵
32	Mongolia, Dornod, 3 km SW of Khukh-Nuur Lake, 49.451°N, 115.494°E	5254	Khukhnur	B6	-	OP765476 ⁵
33	Mongolia, Dornod, Khavirga River, 48.854°N, 115.247°E	4731	Khavirga	B6	ZIN 103850	OP765469 ⁵
		4732	Khavirga	B6	ZIN 103851	OP765470 ⁵
		4733	Khavirga	B6	ZIN 103852	OP765471 ⁵
		4734	Khavirga	B6	ZIN 103853	OP765472 ⁵
		4735	Khavirga	B6	ZIN 103854	OP765473 ⁵
34	Mongolia, Dornod, 20 km NE from Choibalsan, 48.032°N, 114.587°E	4728	ChoibNE	B6	ZIN 103847	OP765466 ⁵
		4729	ChoibNE	B6	ZIN 103848	OP765467 ⁵
		4730	ChoibNE	B6	ZIN 103849	OP765468 ⁵
35	Mongolia, Dornod, 10 km East from Choibalsan, 48.128°N, 114.717°E	5252	ChoibE	B6	-	OP765464 ⁵
		5253	ChoibE	B6	-	OP765465 ⁵
36	Mongolia, Dornod, 20 km SE from Choibalsan, 47.982°N, 114.845°E	4694	ChoibSE	B6	ZIN 103832	OP765461 ⁵
		4695	ChoibSE	B6	ZIN 103833	OP765462 ⁵
		4697	ChoibSE	B6	ZIN 103834	OP765463 ⁵
37	Mongolia, Dornod, 85 km SEE from Choibalsan, 47.747°N, 115.599°E	4699	Choib85	B6	ZIN 103836	OP765460 ⁵
38	Mongolia, Dornod, 25 km NW from Matad, 47.135°N, 115.083°E	4726	Matad	B6	ZIN 103845	OP765446 ⁵
		4727	Matad	B6	ZIN 103846	OP765447 ⁵
39	Mongolia, Dornod, 5 km S from Kolodets Badmashi-Khuduk, 47.184°N, 116.539°E	4722	Badmashi	B6	ZIN 103842	OP765448 ⁵
		4723	Badmashi	B6	ZIN 103843	OP765449 ⁵
		4724	Badmashi	B6	ZIN 103844	OP765450 ⁵
40	Mongolia, Dornod, 10 km NW from Tamsag-Bulak, 47.316°N, 117.2°E	4715	Tamsag	B6	ZIN 103841	OP765451 ⁵
41	Mongolia, Dornod, 14 km S from Buir-Nuur Lake, 47.55°N, 117.71°E	4702	BuirnurS	B6	ZIN 103837	OP765452 ⁵
42	Mongolia, Dornod, Buir-Nuur Lake, 47.7°N, 117.8°E	4151	Buirnur	B6	ZIN 19308	KU184575 ⁴
		4586	Buirnur	B6	ZIN 19307	KU184579 ⁴
		4587	Buirnur	B6	ZIN 19311	KU184580 ⁴
43	Mongolia, Dornod, 5 km NW from Khalkhgol, 47.648°N, 118.564°E	4712	Halhgol	B6	ZIN 103838	OP765453 ⁵
		4713	Halhgol	B6	ZIN 103839	OP765454 ⁵
		4714	Halhgol	B6	ZIN 103840	OP765455 ⁵
44	Mongolia, Dornod, Khalkhgol River, Sumber, 47.59°N, 118.55°E	4153	Sumber	B6	ZIN 19297	KU184577 ⁴
		4585	Sumber	B6	ZIN 19301	KU184578 ⁴
45	China, Inner Mongolia, Ulan-Nur Lake, 48.302°N, 117.480°E	4601	Ulannur	B6	-	OP765456 ⁵
		4602	Ulannur	B6	-	OP765457 ⁵
		4603	Ulannur	B6	-	OP765458 ⁵
		4604	Ulannur	B6	-	OP765459 ⁵
46	Russia, Amur Region, Svobodnensky District, 51.45°N, 127.65°E	3821	Amur	B7	ZIN 41190	KJ192294 ²

Appendix 1. (*termination*)

47	Russia, Amur Region, Romnensky District, Dalnevostochnoye, 50.52°N, 128.84°E	1568	Amur	B7	IBSS 233-08	KJ192291 ²
		1569	Amur	B7	IBSS 234-08	KJ192292 ²
		1570	Amur	B7	IBSS 235-08	KJ192292 ²
		1571	Amur	B7	IBSS 236-08	KJ192293 ²
		1572	Amur	B7	IBSS 2420	KJ192291 ²
		1573	Amur	B7	IBSS 2421	KJ192291 ²
		1574	Amur	B7	IBSS 2426	KJ192293 ²
		1575	Amur	B7	IBSS 2427	KJ192292 ²
		1576	Amur	B7	IBSS 2428	KJ192293 ²
		1577	Amur	B7	IBSS 2429	KJ192292 ²